Zeitschrift: Schweizerische mineralogische und petrographische Mitteilungen = Bulletin suisse de minéralogie et pétrographie

Band: 76 (1996)

Heft: 2

Artikel: Metasomatic tourmalinite formation along basement-cover décollements, Orobic Alps, Italy

Autor: Slack, John F. / Passchier, Cees W. / Zhang, Jia S.

DOI: https://doi.org/10.5169/seals-57697

SCHWEIZ. MINERAL. PETROGR. MITT. 76, 193–207, 1996

Metasomatic tourmalinite formation along basement-cover décollements, Orobic Alps, Italy

by *John F. Slack*[1], *Cees W. Passchier*[2] and *Jia S. Zhang*[3]

Abstract

Cryptocrystalline tourmalinites that occur discontinuously for ~30 km along basement-cover décollements of the Orobic Alps (Italy) formed by the metasomatism of aluminous cataclasites derived from Permian conglomerates and/or feldspathic sandstones. Using Al as an immobile element monitor, calculations show that the majority of tourmalinites in the region formed through the addition of moderate to significant amounts of B, Mg, Na, Sr, and Be, and the loss of moderate to significant Mn, Ca, K, P, Rb, Ba, and Cr; minor Si, Ti, V, light REE, and Eu also were lost. Data for relatively immobile Al, Zr, Th, Sc, Nb, and heavy REE indicate that, on average, these tourmalinites formed through ~12% net mass loss assuming an original conglomerate protolith, or through ~7% net mass loss assuming a sandstone protolith. The B and other introduced constituents in the tourmalinites were deposited by hydrothermal fluids focused along and near basement-cover décollements. These fluids, believed to be associated with late Hercynian felsic magmatism, probably are related to fluids that formed the tourmaline-rich U–Mo–Zn deposits at the nearby Novazza mine and the U–Zn deposits at the nearby Val Vedello mine.

Keywords: tourmalinite, geochemistry, metasomatism, basement-cover décollement, cataclasite, Orobic Alps, Italy.

Introduction

The formation of cataclasites, mylonites, and related rocks commonly involves a variety of textural, mineralogical, and chemical changes (e.g., SIBSON, 1977; SINHA et al., 1986; TOBISCH et al., 1991; CONDIE and SINHA, 1996). Depending on factors such as the nature of the protolith, temperature and pressure conditions, fluid composition, and the time-integrated fluid flux, significant metasomatism may be realized during formation of these rocks. With rare exception (KRAMER and ALLEN, 1954; LABERNARDIÈRE, 1967; BERG, 1977), previous studies of cataclasites and mylonites have not identified abundant tourmaline or anomalous concentrations of boron. We report here on a major and trace element geochemical study of unusual cryptocrystalline tourmaline-rich rocks and tourmalinites that formed by the metasomatism of cataclasites and associated sedimentary rocks along and near basement-cover décollements of the Orobic Alps, northern Italy. The purpose of this paper is to provide a geochemical database for this unusual transformation and an interpretation of related metasomatic effects. Also, because some of the tourmalinites in the Orobic Alps strongly resemble pseudotachylyte in the field and in thin section, the data presented here establish a geochemical framework for distinguishing these tourmalinites from pseudotachylyte.

Geologic setting

The Orobic Alps are characterized by a Variscan metamorphic basement overlain by a volcano-sedimentary cover sequence of Carboniferous to

[1] U.S. Geological Survey, National Center, Mail Stop 954, Reston, Virginia 20192, USA. E-mail: jfslack@GCCMAIL.CR.USGS.GOV.
[2] Institut für Geowissenschaften (Tektonophysik), Johannes Gutenberg-Universität Mainz, Becherweg 21, Postfach 3980, 55099 Mainz, Germany.
[3] Institute of Geology, State Seismological Bureau, P.O. Box 634, 100029 Beijing, China.

Permian age (CASSINIS et al., 1986; CADEL et al., 1987; MILANO et al., 1988). Basement rocks comprise mainly metapelites, metapsammites, and orthogneisses. The metapelites (mica schists) and metapsammites (quartzites) are probably derived from early Paleozoic shales and quartz-rich clastic sediments, respectively; the orthogneisses represent metamorphosed and deformed late Caledonian granitoids and subvolcanic intrusions (CASSINIS et al., 1986). Volumetrically minor basement lithologic units in the region include metagabbro, calcareous metapelite, and marble.

Overlying the basement is a widespread conglomerate unit and a sequence of volcanic and sedimentary rocks that makes up the Carboniferous to Permian Collio Formation (GIOBBI et al., 1981; CADEL, 1986; CASSINIS and PEROTTI, 1993). The conglomerate, of Carboniferous to Early Permian age, consists of quartz and minor basement-rock pebbles and cobbles within upward-fining cycles deposited in a non-marine braided plain environment (CASSINIS et al., 1986). Discontinuous andesitic tuffs occur directly above basement rocks in places (CADEL et al., 1987). Conformably overlying the andesites and conglomerates are rhyolitic volcanic rocks and minor sedimentary rocks (chiefly feldspathic ± micaceous sandstones) of the lower Collio Formation. Rhyolitic volcanic rocks in this sequence consist of multiple cycles of welded ash-flow tuffs (ignimbrites) and lesser airfall tuffs, which were erupted in an extensional half-graben that may represent a caldera-collapse structure (CADEL, 1986; CADEL et al., 1987). Minor andesitic domes and breccia

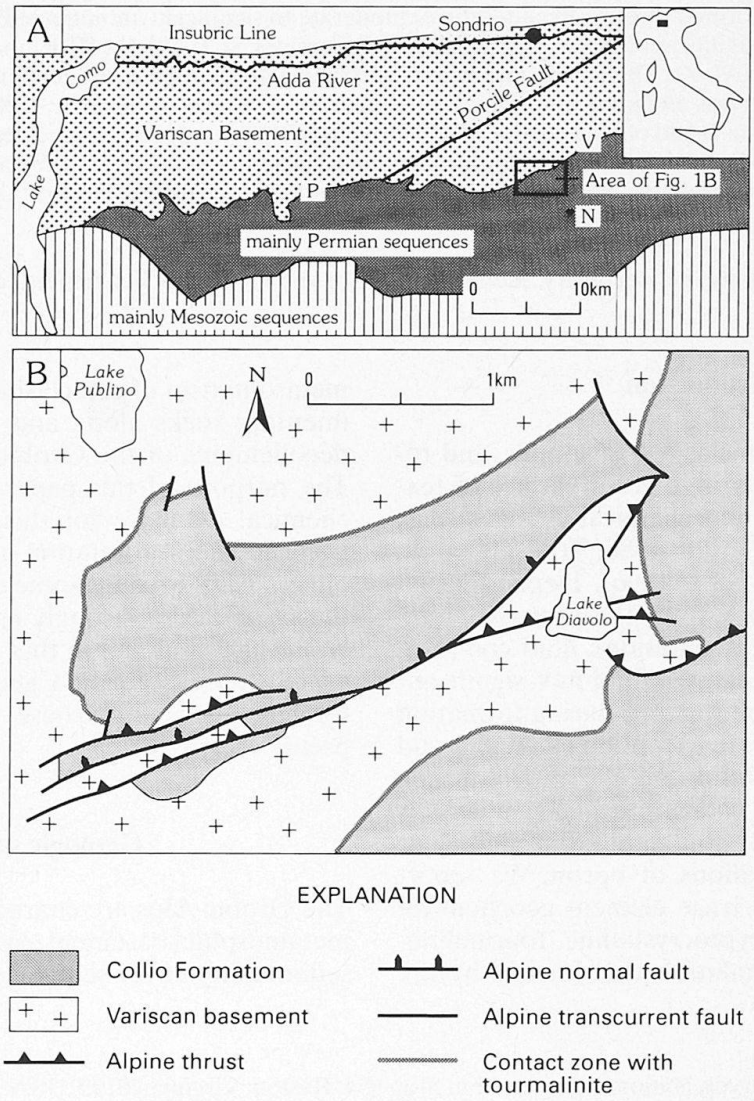

Fig. 1. (A) Simplified geologic map of the Orobic Alps showing location of the study area (box); N = Novazza uranium mine, P = Lake Pescegallo, V = Val Vedello uranium mine. (B) Sketch map of the geology near Lake Publino and Lake Diavolo showing tourmalinite settings. Modified from ZHANG et al. (1994).

pipes occur above the lower Collio. The upper Collio Formation comprises mainly lacustrine and alluvial fan deposits that are unconformably overlain by non-marine fluviatile deposits of the Upper Permian Verrucano Lombardo Formation (CADEL, 1986).

The earliest deformation (D_1 and D_2) in the region produced two generations of pre-Alpine tight to isoclinal folds and related amphibolite-facies assemblages in the Variscan basement (CASSINIS et al., 1986; MILANO et al., 1988; DIELLA et al., 1992). Permian normal faults (D_3) formed as a result of regional extension, preferentially along and near the basement-cover contact (CADEL, 1986; C.W. PASSCHIER and J.-K. BLOM, in prep.). Alpine deformation involved D_4 south-directed thrust faulting of basement over cover rocks, accompanied by reactivation of the extensional normal faults as thrusts; D_5 produced intense ductile shortening and associated low-grade, prehnite-pumpellyite facies metamorphism (MILANO et al., 1988). Deformation during D_5 also developed kilometer-scale upright folds, a slaty cleavage in the Collio Formation, and a crenulation cleavage in basement rocks. South-directed thrust faulting during D_6 was followed locally by late normal faulting. MILANO et al. (1988) recognized two ages of formation of fault rocks in the region, an older pre-Alpine generation of blastomylonites that are folded by F_2 structures, and a younger generation associated with D_4 deformation. The later fault rocks, which occur both in the basement and cover rocks, are aligned at a low angle to F_4 axial structures preferentially near the base of the cover sequence (MILANO et al., 1988). Formation of the younger fault rocks has been related by MILANO et al. (1988) to major decoupling of the cover from the basement during south-directed Alpine thrust faulting (see also DE SITTER and DE SITTER-KOOMANS, 1949; LAUBSCHER, 1985; SCHÖNBORN and SCHUMACHER, 1994).

Tourmalinites

Tourmalinites in the Orobic Alps (Fig. 1) were recently studied by ZHANG et al. (1994) who described their unusual cryptocrystalline (commonly glassy) textures and localization at or near the base of the Collio Formation. These tourmalinites, which in hand specimen resemble dark pseudotachylyte, form discontinuous stratabound lenses < 10 cm thick that extend for ~30 km along Permian normal faults of the basement-cover contact. Some of these normal faults were reactivated during D_4, but the tourmalinite lenses formed prior to this reactivation. The tourmalinites are interlayered with conglomerates, feldspathic sandstones, and thin (< 2 cm thick) cataclasites in contact with, or < 1 m stratigraphically above, basement gneisses (Fig. 2). Contacts between gneiss and immediately overlying cataclasite are sharp, as are those between cataclasite and overlying tourmalinite; tourmalinite-conglomerate contacts, however, are gradational (ZHANG et al., 1994). The tourmalinites display the effects of ductile (e.g., Alpine) deformation, but not of brittle deformation. Whole-rock chemical analyses, X-ray powder diffraction, and transmission electron microscopy have documented ~20–70 modal % of extremely fine-grained (< 0.02 μm) schorl-dravite in these rocks, which together with lesser quartz and sheet silicates form a matrix to angular fragments of quartz and cataclasite (see ZHANG et al., 1994, Fig. 5). Trace to minor amounts (< 5%) of pyrite also occur in the tourmalinites as isolated cubes and/or aggregates. Variable tourmaline (to 10%) is present locally within some of the conglomerates, especially those in contact with the cryptocrystalline tourmalinites. Abundant tourmaline is unknown in the basement rocks, except

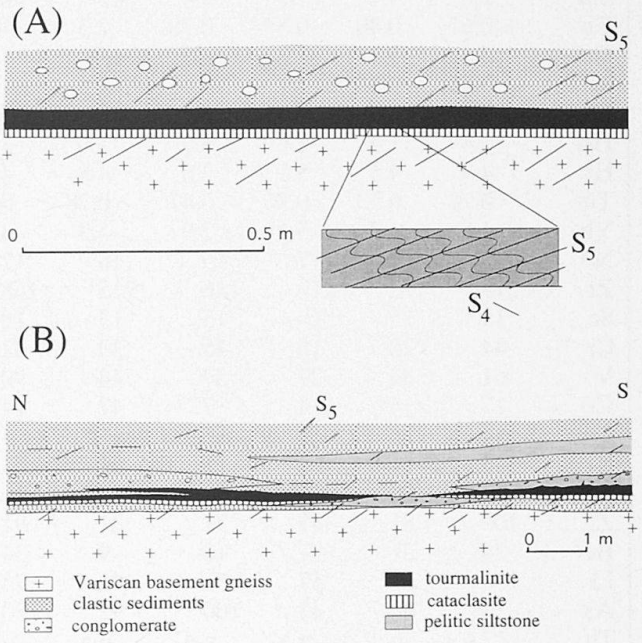

Fig. 2 Sketch showing cross sections of representative tourmalinite occurrences along basement-cover contacts south of Lake Publino. (A) Continuous layers of tourmalinite and cataclasite occur along the the contact zone of basement gneiss and overlying conglomerate. (B) Complex sequence showing several layers of tourmalinite alternating with cataclasite and clastic sediments of the Collio Formation (feldspathic ± micaceous sandstones); note lack of conglomerate above some tourmalinite layers. S_4 and S_5 represent a slaty cleavage and the main foliation, respectively. Modified from ZHANG et al. (1994).

Tab. 1 Representative whole-rock analyses of tourmaline-rich rocks from the Orobic Alps.

No.	2	38B	38C	1542	1577-2	1577-3	1580-2	AD11	AD12	AD15A	AD60A	T13A
						Major elements (wt%)						
SiO_2	64.1	61.2	69.6	61.3	75.8	52.0	59.5	61.5	57.4	57.9	58.0	54.3
TiO_2	0.48	0.34	0.29	0.38	0.44	0.60	0.44	0.80	0.88	0.89	0.38	0.64
Al_2O_3	17.2	18.5	16.3	18.4	11.4	22.1	18.3	17.4	20.7	21.2	18.7	20.7
B_2O_3	4.51	5.15	2.03	5.47	2.32	6.76	6.12	3.22	2.67	3.86	6.44	6.76
$Fe_2O_3^T$	5.01	7.14	3.37	5.94	3.78	8.65	8.05	6.23	5.71	5.17	8.52	9.12
MnO	< 0.01	0.02	< 0.01	< 0.01	< 0.01	0.02	0.02	0.06	0.03	< 0.01	0.02	0.02
MgO	2.68	2.30	1.30	2.78	1.20	3.27	2.70	2.46	2.18	2.54	2.83	3.10
CaO	0.12	0.07	0.03	0.14	0.09	0.19	0.11	0.36	0.47	0.19	0.14	0.14
Na_2O	1.14	1.17	0.40	1.51	1.03	1.89	1.36	0.80	0.73	1.44	1.48	1.55
K_2O	1.09	0.82	3.64	0.95	1.28	0.77	0.32	2.38	4.44	2.70	0.13	0.55
P_2O_5	0.07	0.06	0.06	0.10	0.11	0.09	0.05	0.12	0.11	0.14	0.05	0.07
H_2O	2.33	2.53	2.33	2.44	1.55	2.99	2.53	2.72	3.30	2.94	2.55	2.80
Total	98.73	99.30	99.35	99.41	99.00	99.33	99.50	98.05	98.62	98.97	99.24	99.75
						Trace elements (ppm)						
Rb	63	46	215	49	68	42	15	132	255	144	11	33
Sr	200	170	62	120	84	280	250	140	140	140	310	260
Ba	98	68	140	90	56	75	77	230	420	280	43	51
Y	37	40	46	24	44	40	41	26	33	31	50	44
La	19	34	45	35	160	32	49	18	42	29	22	30
Ce	35	57	86	68	320	63	96	35	71	51	42	60
Nd	14	18	32	27	130	28	41	13	26	18	17	26
Sm	3.8	4.7	7.9	5.4	23	6.9	9.1	3.3	5.9	4.7	4.4	5.9
Eu	0.67	0.40	0.57	0.78	3.3	1.3	0.93	0.88	1.2	1.1	0.53	1.1
Gd	5.1	5.3	7.3	4.5	11	7.6	7.6	4.5	6.0	5.9	5.5	7.3
Tb	0.96	0.85	1.1	0.66	1.5	1.1	1.1	0.78	0.93	0.96	1.0	1.3
Dy	7.1	6.5	8.3	5.1	8.8	7.7	8.2	5.2	6.3	5.7	7.4	7.8
Ho	1.4	1.4	1.6	1.0	1.6	1.4	1.5	1.2	1.2	1.1	1.6	1.7
Er	4.4	4.5	5.1	2.8	4.8	4.5	4.6	3.3	4.0	3.4	4.3	4.9
Tm	0.72	0.73	0.76	0.47	0.78	0.68	0.61	0.55	0.57	0.54	0.71	0.75
Yb	4.5	4.7	5.1	2.9	5.3	4.4	4.5	3.5	3.6	3.9	4.9	5.2
Nb	22	14	17	15	18	17	19	15	18	15	18	20
Zr	215	172	210	146	215	168	180	194	265	245	172	200
Sc	15	15	16	15	13	18	16	18	18	19	16	21
Cr	44	28	18	35	33	62	41	120	99	110	27	58
V	61	34	27	57	44	90	47	130	100	130	39	82
Co	17	< 4	< 4	7	42	14	12	19	17	25	8	18
Cu	< 4	15	5	5	11	< 4	9	65	< 4	7	< 4	< 4
Ni	45	11	< 8	15	51	53	21	64	64	62	16	58
Pb	< 20	30	< 20	21	< 20	< 20	23	< 20	< 20	19	25	21
Zn	100	81	47	31	31	81	88	55	62	59	80	100
Be	24	21	7	18	9	34	35	16	15	21	37	31
Li	100	61	57	51	41	75	73	61	54	59	77	50
As	54	80	43	100	92	130	140	70	< 40	92	140	130
Th	17.6	n.a.	n.a.	n.a.	n.a.	n.a.	n.a.	n.a.	n.a.	16.5	n.a.	n.a.
U	22.8	n.a.	n.a.	n.a.	n.a.	n.a.	n.a.	n.a.	n.a.	4.4	n.a.	n.a.

Sample descriptions and locations: 2 = fine-grained tourmalinite from west of Lake Diavolo; 38B = fine-grained tourmalinite from west of Lake Diavolo; 38C = tourmaline-rich conglomerate from west of Lake Diavolo; 1542 = fine-grained tourmalinite from near Lake Pescegallo; 1577-2 = tourmaline-rich cataclasite from south of Lake Publino; 1577-3 = fine-grained tourmalinite from south of Lake Publino; 1580-2 = fine-grained tourmalinite from south of Lake Publino; AD11 = fine-grained tourmalinite from east of Lake Diavolo; AD12 = fine-grained tourmalinite from east of Lake Diavolo; AD15A = fine-grained tourmalinite from north of Lake Diavolo; AD60A = fine-grained tourmalinite from west of Lake Diavolo; T13A = fine-grained tourmalinite from south of Lake Publino. Note: Total iron as Fe_2O_3; n.a. = not analyzed; Nos AD11, AD12, AD15A = Group B, others Group A.

Tab. 2 Representative whole-rock analyses of basement and cover rocks from the Orobic Alps.

No.	1577-1	JK-24	AD37	AM13	AD42	JK18	JK21	T2	JK19	JK20	1559	JK23
						Major elements (wt %)						
SiO_2	80.4	86.6	75.4	78.8	60.0	64.8	69.4	62.3	59.4	62.0	68.5	62.5
TiO_2	0.08	0.05	0.81	0.70	1.0	0.83	0.62	0.93	0.96	1.06	0.52	0.67
Al_2O_3	10.7	6.78	11.2	10.3	20.9	17.3	12.9	22.2	19.1	19.6	15.1	13.4
B_2O_3	0.06	0.04	0.04	0.04	0.03	0.07	0.61	0.14	0.77	0.19	0.22	0.20
$Fe_2O_3^T$	1.38	1.71	3.89	2.75	3.34	5.72	6.94	2.12	6.05	4.61	4.50	6.28
MnO	< 0.01	0.03	0.03	0.03	0.02	0.07	0.16	< 0.01	0.09	0.05	0.04	0.24
MgO	0.53	0.59	1.56	0.82	2.03	1.03	1.01	1.00	1.44	1.08	0.76	2.14
CaO	0.31	0.23	0.70	0.21	0.24	0.18	0.21	0.10	0.60	0.21	0.03	2.36
Na_2O	0.40	0.28	2.17	1.42	< 0.15	1.11	0.41	0.79	0.35	0.49	< 0.15	< 0.15
K_2O	3.59	2.04	1.61	2.51	7.10	4.62	3.72	6.54	5.66	6.36	4.85	4.42
P_2O_5	0.25	0.16	0.22	0.13	0.18	0.13	0.16	0.11	0.14	0.16	0.12	0.20
H_2O	1.58	1.37	1.97	1.48	4.05	3.36	3.03	3.23	3.46	3.39	4.90	2.78
Total	99.28	99.88	99.60	99.19	98.89	99.16	99.17	99.46	98.02	99.20	99.54	99.09#
						Trace elements (ppm)						
Rb	220	122	64	87	330	225	210	330	315	355	260	260
Sr	14	11	120	110	24	66	42	54	74	43	41	69
Ba	150	120	440	530	1700	540	350	620	540	630	410	350
Y	10	< 8	21	20	39	23	20	25	27	29	28	21
La	9.2	4.2	39	42	68	48	27	52	42	69	51	28
Ce	17	8.2	78	83	130	88	47	93	77	130	100	49
Nd	8.9	4.2	28	32	49	35	19	34	30	54	42	21
Sm	3.0	0.97	5.7	6.0	10	6.6	3.7	6.5	6.3	11	8.5	4.1
Eu	0.69	0.18	1.2	1.3	2.6	1.5	0.93	1.3	1.4	2.0	2.2	1.1
Gd	3.1	1.2	4.8	5.4	9.7	6.0	3.9	6.1	6.2	8.5	6.8	4.8
Tb	0.43	0.22	0.65	0.66	1.3	0.84	0.64	0.80	0.86	1.2	0.80	0.67
Dy	2.0	1.3	3.9	4.3	7.1	5.2	4.1	5.0	6.0	6.8	5.4	4.1
Ho	0.36	0.20	0.73	0.84	1.5	0.89	0.79	0.93	1.1	1.3	0.98	0.83
Er	1.1	0.60	2.2	2.5	4.4	2.7	2.6	2.9	3.3	3.9	3.3	2.3
Tm	0.14	0.06	0.31	0.37	0.72	0.40	0.37	0.39	0.50	0.59	0.41	0.32
Yb	1.1	0.58	2.3	2.5	5.3	2.4	2.5	2.8	3.1	4.2	3.0	2.3
Nb	14	< 10	12	12	16	16	16	18	18	18	18	11
Zr	63	32	325	485	240	158	162	192	186	290	250	174
Sc	< 8	< 8	11	< 8	23	14	12	19	17	15	13	14
Cr	4	4	67	48	140	98	70	120	120	88	44	79
V	11	< 8	72	47	160	90	75	120	100	90	44	110
Co	7	< 4	4	8	< 4	15	16	4	12	5	4	16
Cu	< 4	49	15	< 4	12	< 4	72	< 4	< 4	5	< 4	58
Ni	18	< 8	20	15	16	39	35	13	42	21	28	25
Pb	< 20	< 20	< 20	54	< 20	< 20	< 20	27	< 20	< 20	< 20	25
Zn	8	17	46	310	23	59	41	11	39	27	62	23
Be	< 4	< 4	< 4	< 4	7	< 4	6	5	7	6	5	4
Li	43	33	31	27	60	56	35	79	41	49	81	40
As	< 40	< 40	40	< 40	< 40	< 40	50	< 40	< 40	< 40	< 40	64
Th	n.a.	n.a.	19.9	n.a.	15.3	n.a.	n.a.	18.9	n.a.	n.a.	n.a.	n.a.
U	n.a.	n.a.	3.2	n.a.	4.9	n.a.	n.a.	6.0	n.a.	n.a.	n.a.	n.a.

Sample descriptions and locations: 1577-1 = basement gneiss from south of Lake Publino; JK-24 = basement gneiss from east of Lake Diavolo; AD37 = basement schist from west of Lake Diavolo; AM13 = basement schist from east of Ca. S. Marco; AD42 = basement pseudotachylyte from southwest of Lake Publino; JK18 = conglomerate from east of Lake Diavolo; JK21 = conglomerate from east of Lake Diavolo; T2 = conglomerate from south of Lake Publino; JK19 = Collio Formation feldspathic sandstone from east of Lake Diavolo; JK20 = Collio Formation feldspathic sandstone from east of Lake Diavolo; 1559 = Collio Formation foliated volcanic from southeast of Lake Diavolo; JK23 = calcareous Collio Formation pyroclastic from east of Lake Diavolo. Note: Total iron as Fe_2O_3; n.a. = not analyzed. #Includes 3.90 wt% CO_2 from loss on ignition.

for one cataclasite south of Lake Publino that contains ~12 modal %.

Other tourmaline concentrations in the region have been described by CADEL et al. (1987), FUCHS (1987), FUCHS (1989), and FUCHS and MAURY (1995). At the Novazza uranium mine (Fig. 1), abundant tourmaline occurs locally in disseminations, veins, and stratabound lenses within rhyolitic ignimbrites of the Collio Formation. The nearby Val Vedello uranium mine lacks tourmaline concentrations, but contains boron enrichments (to 5000 ppm) in albite-rich cataclasites present in mylonitic zones along the basement-cover contact (FUCHS and MAURY, 1995); tourmaline also occurs along this contact 400 m east of the mine (Y. Fuchs, pers. commun. to JFS, 1996). CADEL et al. (1987) additionally reported abundant tourmaline near andesitic intrusive bodies in the region, and locally pervasive tourmalinization of fine-grained volcanic ash beds and sandstones of the Collio Formation at and near the Novazza mine.

Geochemistry

Whole-rock analyses of 12 tourmaline-rich rocks and 23 tourmaline-poor basement and cover rocks were acquired by X-ray fluorescence (major elements, Rb, Nb, and Zr), inductively coupled plasma-atomic emission spectrometry (B, Sr, Ba, Y, Sc, Cr, V, Co, Cu, Ni, Pb, Zn, Be, Li, As), inductively coupled plasma-mass spectrometry (La, Ce, Nd, Sm, Eu, Gd, Tb, Dy, Ho, Er, Tm, Yb), and optical emission spectrometry (Sn, W). Fifteen samples were also analyzed for a broad suite of trace elements by instrumental neutron activation methods; only data for Th and U are presented here[1]. Representative analyses for all major rock types are given in tables 1 and 2. The tourmalinites show distinctive major-element compositions including B_2O_3 contents of 2.03–6.76 wt%. These rocks are also characterized by a wide range of values for SiO_2 (52.0–75.8 wt%), Al_2O_3 (11.4–22.1 wt%), $Fe_2O_3^T$ (3.37–9.12 wt%), and K_2O (0.13–4.44 wt%); amounts of MgO (1.20–3.27 wt%), CaO (0.03–0.47), and Na_2O (0.40–1.89 wt%) show smaller variations. By comparison, samples of basement schist and gneiss, and of overlying conglomerate, clastic sediment (feldspathic sandstone), and andesitic rock have higher SiO_2 and K_2O, and lower Al_2O_3, $Fe_2O_3^T$, and MgO than the tourmalinites (Figs 3A–C). TiO_2 contents of the tourmalinites fall into two populations, one defined by 0.34–0.64 wt% ($n = 7$) designated as Group A, and another by 0.80–0.89 wt% ($n = 3$) from the Lake Diavolo area that are designated as Group B.

Trace element concentrations of the tourmalinites overlap those of surrounding basement and cover rocks (Tabs 1, 2). Group A tourmalinites contain low Rb (11–63 ppm), whereas the Group B tourmalinites have 132–255 ppm Rb; conglomerates and sandstones contain 190–355 ppm Rb, and basement schists and gneisses have 54–87 and 38–220 ppm Rb, respectively. A strong correlation between Rb and K_2O (Fig. 3C) suggests that the Rb is contained within muscovite. Excluding schist sample AD37 (120 ppm), Sr values are consistently higher in both Group A and Group B tourmalinites (120–310 ppm) than in any other rocks of the study area (conglomerates and sandstones contain 31–74 ppm Sr). Ba contents vary from 43–98 ppm in Group A tourmalinites and 230–420 ppm in Group B tourmalinites, and overall are broadly similar to those of their surrounding country rocks.

Concentrations of ferromagnesian and high field strength elements display diverse patterns. Cr, for example, shows a large variation and broad correlation with TiO_2 (Fig. 3D), in which Group A tourmalinites contain 27–62 ppm and Group B tourmalinites 99–120 ppm. Values for Sc and V range from 15–21 and 34–130 ppm, respectively, and are similar to those for surrounding basement and cover rocks. Nb and Zr contents are not systematically different among the various lithologic series analyzed. Concentrations of Y, however, are generally higher in the tourmalinites and tourmaline-rich conglomerates (31–52 ppm), as are those of Yb (Fig. 3E). A correlation of Y with Yb (Fig. 3F) implies that these elements are contained in accessory monazite and/or allanite that were relatively resistant to dissolution during cataclasis and metamorphism.

Some of the tourmalinites are enriched in Be, As, and U relative to their country rocks. The tourmalinites contain 7–37 ppm Be (avg 22 ppm), compared to a maximum of 7 ppm Be in gneisses, schists, pseudotachylytes, conglomerates, and sandstones. Concentrations of As in the tourmalinites vary from 43–140 ppm (avg ~92 ppm) relative to a maximum of 64 ppm (avg < 40 ppm) in tourmaline-poor country rocks, the higher As probably residing in minor disseminated pyrite present in the tourmalinites. Reconnaissance data also show concentrations of U in some of the tour-

[1] Among the 35 samples analyzed in detail for this study, only five were submitted for determination of U, Th, and other trace elements by instrumental neutron activation analysis (INAA); 10 additional samples from the region were also analyzed by INAA but a complete database for them was not acquired because sufficient material for analysis was not available.

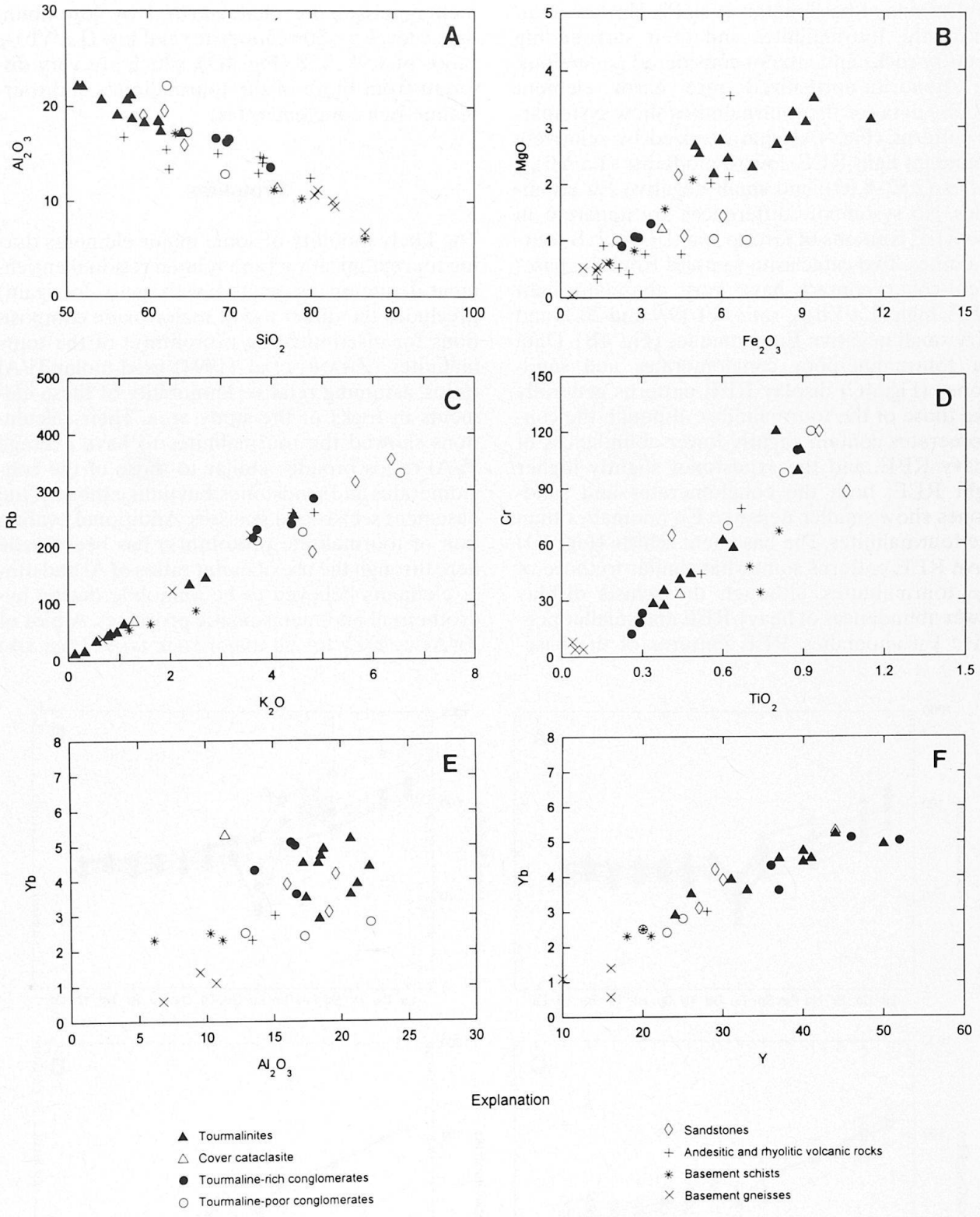

Fig. 3 Variation diagrams showing correlations of whole-rock analytical data. (A) SiO_2 vs Al_2O_3; (B) Fe_2O_3 vs MgO; (C) K_2O vs Rb; (D) TiO_2 vs Cr; (E) Al_2O_3 vs Yb; (F) Y vs Yb. Major element values in wt%, trace elements in ppm; Fe_2O_3 in (B) is total iron. Data for volcanic rocks from this study and CADEL (1986).

malinites (e.g., 22.8 ppm, sample 2, Tab. 1) and in one cataclasite from south of Lake Publino in contact with tourmalinite (sample T4B-2, 226 ppm; C.W. Passchier and J.S. Zhang, unpub. data). Sn and W contents are below detection limits of 10 and 20 ppm, respectively, for all samples analyzed, except for one tourmalinite from south of Lake Publino (1580-2) that contains 30 ppm W. Con-

centrations of base metals (Cu, Pb, Zn) are similar in the tourmalinites and their surrounding country rocks and are not considered anomalous.

Chondrite-normalized rare earth element (REE) data for the tourmalinites show systematic patterns (Fig. 4A) characterized by relatively abundant light REE, low to moderate $(La/Yb)_{CN}$ ratios (2.82–8.05), and small negative Eu anomalies. No systematic differences are apparent in the REE contents of Group A and Group B tourmalinites. Two cataclasite samples from the basement-cover contact have very abundant light REE, high $(La/Yb)_{CN}$ ratios of 19.9 and 20.1, and very small negative Eu anomalies (Fig. 4B). Data for tourmaline-poor conglomerates and sandstones (Fig. 4C) display REE patterns generally like those of the tourmalinites, although the conglomerates contain slightly lower abundances of heavy REE, and the sandstones slightly higher light REE; both the conglomerates and sandstones show smaller negative Eu anomalies than the tourmalinites. The basement schists (Fig. 4D) have REE patterns somewhat similar to those of the tourmalinites, although the schists display lower abundances of heavy REE and smaller negative Eu anomalies. REE patterns of the basement gneisses are characterized by low abundance levels (< 20x chondrite) and low $(La/Yb)_{CN}$ ratios of 1.95–5.58 (Fig. 4D), which are very different from those of the tourmalinites and tourmaline-rich conglomerates.

Protoliths

The likely mobility of some major elements during tourmalinization (and related residual enrichment/depletion associated with mass loss/gain) precludes the direct use of major oxide compositions for discriminating protolith(s) of the tourmalinites. ZHANG et al. (1994) used molar Ti/Al ratios, assuming relative immobility of these elements in rocks of the study area. Their calculations showed the tourmalinites to have average Ti/Al ratios broadly similar to those of the conglomerates and sandstones, but unlike those of the basement schists and gneisses. Additional evaluation of tourmalinite protolith(s) has been made here through the use of molar ratios of Al and other elements believed to be immobile during hydrothermal and metasomatic processes. A plot of Zr/Al vs Y/Zr for all major rock types (Fig. 5A)

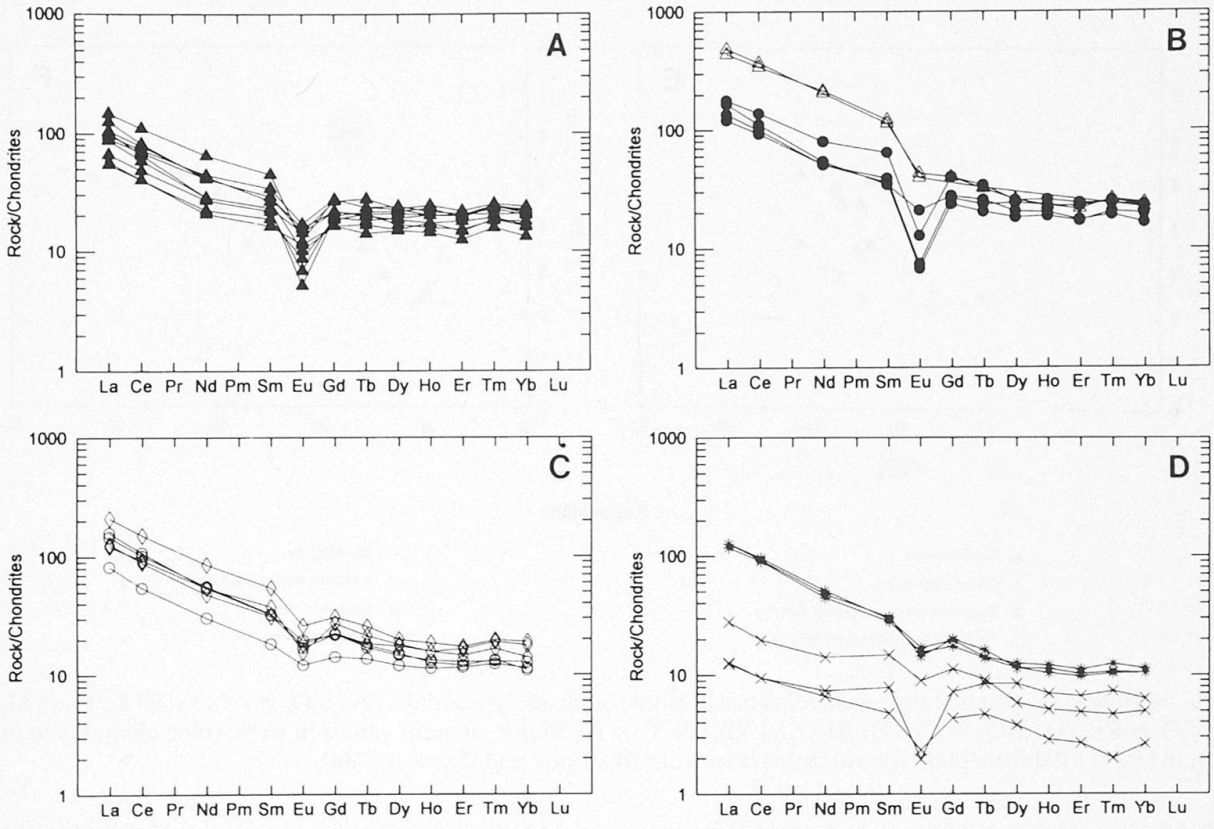

Fig. 4 Chondrite-normalized plots of rare earth element data. (A) tourmalinites; (B) cover cataclasites and tourmaline-rich conglomerates; (C) tourmaline-poor conglomerates and sandstones; (D) tourmaline-poor basement schists and gneisses. Chondrite data from NAKAMURA (1974). Symbols as in figure 3.

shows that, excepting one sample of basement gneiss, the only lithologic units similar to the tourmalinites are the volcanic rocks, conglomerates, and sandstones. Data for Collio Formation volcanics show Y/Zr ratios that range from < 0.22 for andesites, to > 0.22 for rhyolites. Andesites can be ruled out as protoliths in most cases based on their geologic occurrence as local discontinuous units, and rhyolites based on their stratigraphic distribution well above the basement-cover contact (Fig. 1; see also CADEL et al., 1987). Gneiss sample 1577-1 has a relatively low Y/Zr ratio (0.16) like that of some tourmalinites, but unlike that of adjacent tourmalinite sample 1577-3 (0.24). Gneisses are also precluded as protoliths because of their lower Sc/Al ratios (Fig. 5B), and their Th/Al ratios of 0.16–0.23 relative to those of the tourmalinites (0.34–0.45); tourmaline-free conglomerates have Sc/Al ratios of 1.82–2.09 and Th/Al ratios of 0.37–0.40, in the range of the tourmalinites. The schists cannot be protoliths based on their low Y/Zr and high Zr/Al ratios. Overall, these data suggest that the tourmalinites were derived from conglomerates and/or sandstones of the cover sequence, and not from the basement schists or gneisses (or Collio Formation volcanics). The presence of quartz fragments in the tourmalinites, and quartz pebbles and cobbles in the conglomerates, further suggests that the protolith of most of the tourmalinites was conglomerate (ZHANG et al., 1994). However, because some of the tourmalinites lack directly associated conglomerate and are in contact with sandstones (Fig. 2B), they probably have a sandstone protolith.

The extremely fine-grained nature of the tourmalinites provides an additional constraint on their origin. No other rocks in the study area have such aphanitic textures except for basement cataclasites and pseudotachylytes, and cataclasites occurring along the basement-cover contact ("cover" cataclasites). The basement cataclasites and pseudotachylytes cannot be protoliths of the tourmalinites because of their restricted occurrence and commonly deformed nature (cf. MILANO et al., 1988). The cover cataclasites, however, are attractive as protoliths because they form semicontinuous narrow layers between the gneisses and tourmalinites, and display similar cryptocrystalline textures (ZHANG et al., 1994, Fig. 3). Such cataclasites thus represent the most probable direct precursors of the tourmalinites. Because of their thin (<2 cm) geometry these cover cataclasites are very difficult to sample without contamination from adjacent lithologic members (gneiss and tourmalinite), and our only completely analyzed sample (1577-2, Tab. 1) unfortunately contains significant B_2O_3. This cover cataclasite

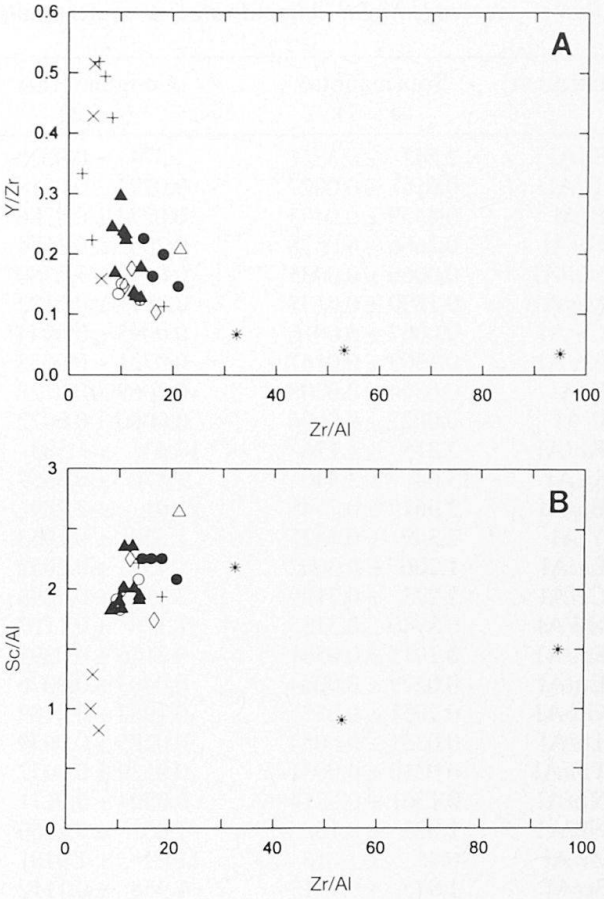

Fig. 5 Immobile element ratio plots discriminating protoliths of tourmalinites. (A) Zr/Al vs Y/Zr; (B) Zr/Al vs Sc/Al. All data based on molar element values. Symbols as in figure 3.

nevertheless displays immobile-element geochemical signatures generally like those of the tourmaline-poor conglomerates and sandstones of the study area, although it has greater light REE abundances (Fig. 4B) and a slightly higher Zr/Al ratio (Figs 5A, B). The gneisses, by comparison, have lower average Sc/Al and Zr/Al and higher average Y/Zr, and the gneiss in direct contact with this cataclasite (1577-1) has a lower Sc/Al ratio of 0.84 and a higher Y/Zr ratio of 0.43 relative to the Sc/Al and Y/Zr ratios of 2.56 and 0.21 calculated for the adjoining cataclasite, and 1.83 and 0.23 calculated for the adjoining tourmalinite (sample 1577-3). A detailed geochemical study of the cover cataclasites would be necessary to rigorously evaluate their protolith(s), which is beyond the scope of this paper. However, available data suggest that the cataclasites along the basement-cover contact most likely derive from the conglomerates and/or sandstones, and not the gneisses. If this interpretation is correct, then the typical fine-grained tourmalinites of the study area must have formed from previously cata-

Tab. 3 Average molar element ratios of tourmalinites, conglomerates, and sandstones from the Orobic Alps.*

Element	Tourmalinite ($n = 7$)	Conglomerate ($n = 3$)	Sandstone ($n = 3$)	Tourmalinite/ Conglomerate	Tourmalinite/ Sandstone
Si/Al	2.542 ± 0.3821	3.374 ± 0.9022	2.913 ± 0.3558	0.7533	0.8728
Ti/Al	0.0151 ± 0.0027	0.0293 ± 0.0018	0.0276 ± 0.0080	0.5161	0.5477
B/Al	0.4439 ± 0.0407	0.0274 ± 0.0280	0.0261 ± 0.0224	16.21	17.01
Fe/Al	0.2666 ± 0.0538	0.2052 ± 0.1154	0.1759 ± 0.0213	1.299	1.516
Mn/Al	0.0069 ± 0.0035	0.0410 ± 0.0380	0.0260 ± 0.0062	0.1688	0.2659
Mg/Al	0.1899 ± 0.0133	0.0771 ± 0.0172	0.1122 ± 0.0433	2.463	1.693
Ca/Al	0.0067 ± 0.0016	0.0095 ± 0.0044	0.0219 ± 0.0086	0.7048	0.3047
Na/Al	0.1303 ± 0.0167	0.0721 ± 0.0238	0.1513 ± 0.1636	1.806	0.8613
K/Al	0.0324 ± 0.0208	0.3067 ± 0.0128	0.3325 ± 0.0134	0.1057	0.0975
P/Al	0.0027 ± 0.0006	0.0060 ± 0.0022	0.0058 ± 0.0004	0.4469	0.4585
Rb/Al	2.315 ± 1.176	17.43 ± 1.583	18.24 ± 3.113	0.1328	0.1269
Sr/Al	13.64 ± 3.440	3.570 ± 0.5557	2.822 ± 0.6343	3.822	4.835
Ba/Al	2.961 ± 0.7948	21.91 ± 2.289	22.71 ± 1.513	0.1352	0.1304
Y/Al	2.349 ± 0.4425	1.520 ± 0.1953	1.800 ± 0.2352	1.545	1.305
La/Al	1.206 ± 0.3662	1.751 ± 0.2052	1.987 ± 0.4185	0.6884	0.6068
Ce/Al	2.273 ± 0.7199	3.111 ± 0.4298	3.769 ± 0.7856	0.7307	0.6031
Nd/Al	0.8940 ± 0.3155	1.176 ± 0.1727	1.502 ± 0.3446	0.7601	0.5951
Sm/Al	0.2015 ± 0.0581	0.2156 ± 0.0291	0.3051 ± 0.0653	0.9345	0.6605
Eu/Al	0.0279 ± 0.0084	0.0483 ± 0.0076	0.0553 ± 0.0089	0.5792	0.5054
Gd/Al	0.2051 ± 0.0335	0.1982 ± 0.0189	0.2620 ± 0.0404	1.035	0.7828
Tb/Al	0.0331 ± 0.0054	0.0285 ± 0.0039	0.0357 ± 0.0052	1.160	0.9270
Tm/Al	0.0210 ± 0.0031	0.0139 ± 0.0027	0.0183 ± 0.0024	1.512	1.147
Yb/Al	0.1361 ± 0.0214	0.0894 ± 0.0171	0.1204 ± 0.0201	1.522	1.131
Nb/Al	1.023 ± 0.1838	1.081 ± 0.1966	1.056 ± 0.0697	0.9470	0.9693
Zr/Al	10.45 ± 1.616	11.22 ± 1.918	13.08 ± 2.429	0.9311	0.7988
Sc/Al	1.945 ± 0.1513	1.958 ± 0.1112	1.982 ± 0.2135	0.9987	0.9817
Cr/Al	4.239 ± 1.037	10.71 ± 0.2238	9.564 ± 1.808	0.3960	0.4432
V/Al	6.000 ± 1.636	10.88 ± 0.4993	9.598 ± 0.4895	0.5516	0.6251
Ni/Al	2.761 ± 1.525	3.189 ± 1.573	2.615 ± 0.8149	0.8657	1.056
Zn/Al	6.504 ± 1.843	3.653 ± 2.045	7.217 ± 6.505	1.780	0.9012
Be/Al	16.72 ± 3.832	3.017 ± 1.636	2.966 ± 1.137	5.542	5.636
Li/Al	53.63 ± 14.90	46.23 ± 5.139	61.88 ± 39.88	1.160	0.8675

* Major element data based on bulk compositions recalculated to 100% on a volatile-free basis; uncertainties shown are 1σ values. Note: Na data for sandstones are strongly affected by one albite-rich sample.

clasized conglomerates and/or sandstones, as these precursors best explain the observed geochemical and textural features of the tourmalinites.

Mass changes

The clastic sedimentary (conglomerate/sandstone) protolith identified for the tourmaline-rich rocks precludes the use of standard mass-balance calculations to quantify gains and losses of elements during tourmalinization. Unlike granitoids and volcanic rocks that chemically may be relatively homogeneous and thus suitable for quantitative mass-balance studies, clastic sediments commonly show a large range of major and trace element concentrations due to sorting and other sedimentary processes (e.g., SAWYER, 1986; ARGAST and DONNELLY, 1987). As a result, any calculation of a single unaltered protolith composition for a suite of clastic sediments will, in most cases, yield an unacceptably large uncertainty (see AGUE, 1994). The approach taken here is to calculate relative mass changes using Al as an immobile reference element. Such an approach is considered reasonable given the documented immobility of Al during most hydrothermal and metamorphic processes, including those involving shear zones, cataclasites, and tourmalinites (e.g., KERRICH et al., 1977; FERRY, 1979; MARQUER et al., 1985; SLACK et al., 1993; GUNDERSEN and GATES, 1995; CONDIE and SINHA, 1996). General immobility of Al in rocks of the study area is also suggested by broad correlations between Al_2O_3 and Yb for most of the tourmaline-rich rocks and their unaltered (tourmaline-poor) precursor sediments (Fig. 3E), and by its coherent behavior relative to

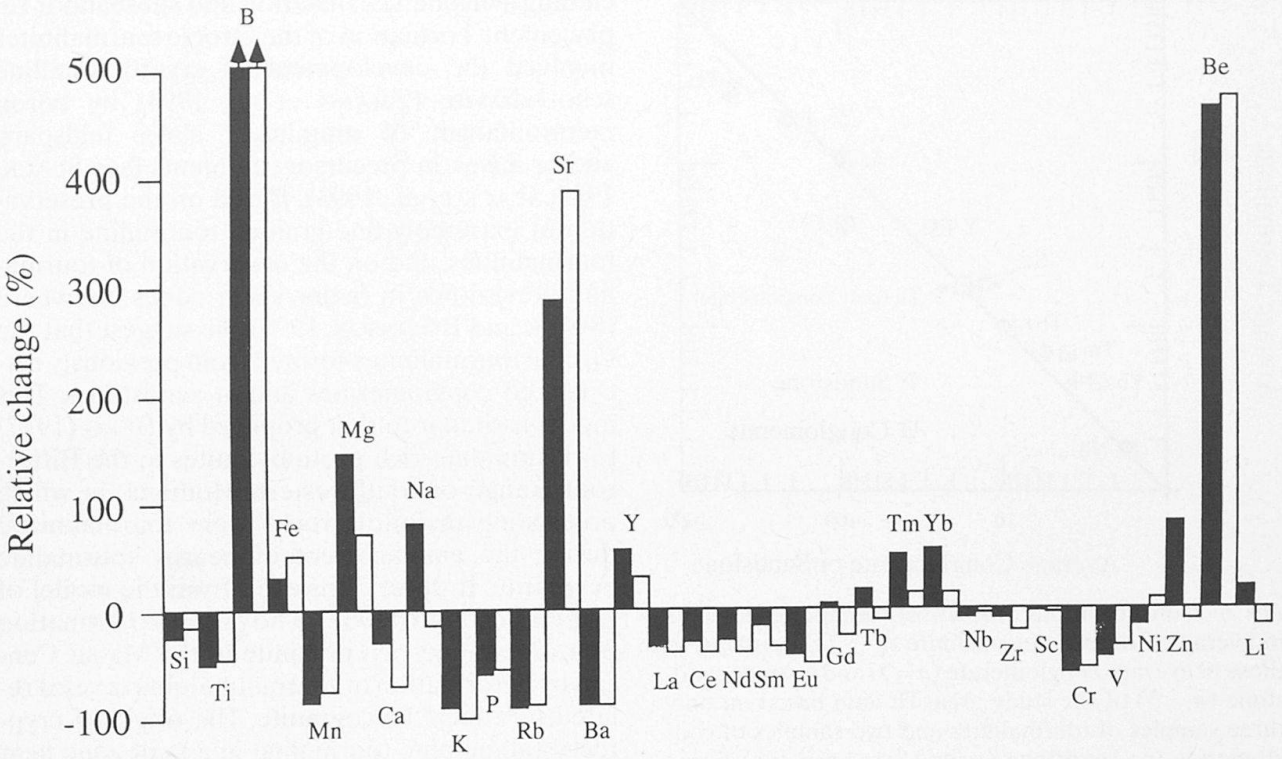

Fig. 6 Relative change (in percent) of elements in average Group A tourmalinite ($n = 7$) compared to those in protoliths of average conglomerate ($n = 3$) shown by the black bars, and of average sandstone ($n = 3$) shown by the open bars. Data based on molar element compositions recalculated on a volatile-free basis, and normalized to average molar Al values (see Tab. 3).

other characteristically immobile elements including Zr, Y, Nb, Th, Sc, and other heavy REE. Table 3 lists average molar element ratios of the more common Group A tourmalinites compared to those of tourmaline-poor conglomerates and sandstones. The Group A tourmalinites consistently display the greatest amount of chemical change relative to their precursor sediments, and are emphasized here; Group B tourmalinites are characterized by less change and are not discussed further. Compared to average data for the conglomerates and sandstones, the Group A tourmalinites display moderate to significant (> 50%) addition of B, Mg, Na[2], Sr, and Be, and minor addition (10–50%) of Fe, Y, Tm, Yb, and Zn (Fig. 6). Moderate to significant loss (> 50%) is shown by Mn, Ca, K, P, Rb, Ba, and Cr; Si, Ti, La, Ce, Nd, Sm, Eu, Zr, and V display minor (10–50%) loss. Relative changes for Gd, Tb, Nb, Sc, Ni, and Li are not significant (± 10% or less). In general, changes calculated using a conglomerate protolith are similar to those for a sandstone protolith, although some discrepancies occur for Ca, Na, Gd, Tb, Tm, Yb, Ni, Zn, and Li. Use of a sandstone protolith results in a more consistent pattern in which most of these elements (especially the heavy REE) are essentially immobile. Adapting the recently devised least-squares method of BAUMGARTNER and OLSEN (1995) for the relatively immobile elements Al, Zr, Th, Sc, Nb, and the heavy REE, a net mass loss of ~12% is calculated for the average Group A tourmalinite relative to a conglomerate protolith; a lower net mass loss of ~7% is obtained using a sandstone protolith (Fig. 7). These calculated net mass losses for tourmalinite formation are also consistent with the distribution of data for Y and Yb in tourmalinites, conglomerates, and sandstones of the study area (Fig. 3F), in which the higher concentrations of Y and Yb in the tourmalinites, relative to their precursor sediments, reflect an increase in resistant accessory monazite + zircon ± allanite due to removal of other components (chiefly K and Ca). Other enrichments in immobile elements, relative to tourmaline-poor

[2] The Na value calculated assuming a sandstone protolith is strongly affected by one albite-rich sample. Inclusion of this sample in the average (Tab. 3; Fig. 6) yields a relative change of –14%; exclusion of this sample yields a relative change of +266%, which is more consistent with the value obtained using a conglomerate protolith. Considered overall, Na in the tourmalinites shows an increase relative to its clastic sedimentary precursors.

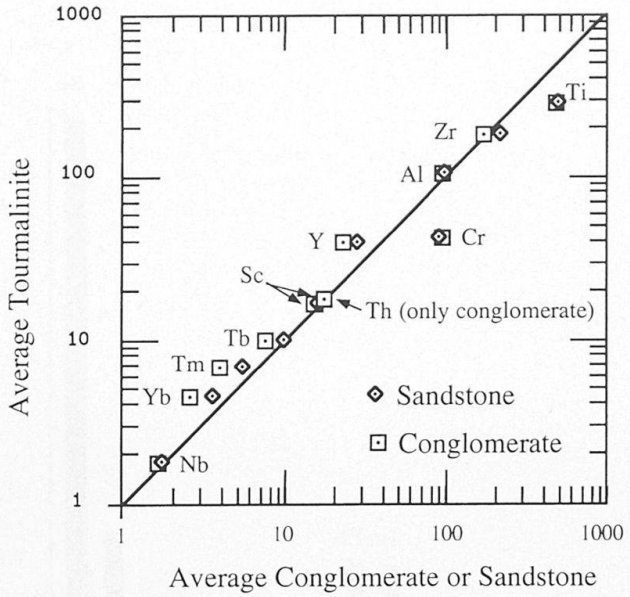

Fig. 7 Concentrations of relatively immobile elements in average Group A tourmalinite (n = 7) compared to those of average conglomerate (n = 3) and average sandstone (n = 3) of the study area; Th data based on only three samples of tourmalinite and two samples of conglomerate (no sandstone analyses are available). Some values are scaled to fit; calculations were made using unscaled values. Note proximity of data for average sandstone to 1:1 line of equal composition and zero net mass change, and systematic shifts to lower concentrations in conglomerates (open squares) relative to sandstones (open diamonds). Conglomerate protolith requires ~12% net mass loss; sandstone protolith requires ~7% net mass loss (see text).

sandstone and conglomerate (Tab. 3), are due to the overall net mass loss associated with tourmalinite formation (cf. MACLEAN and BARRETT, 1993; SLACK, 1996). Because of the density increase involved in the transformation of quartzose cataclasite (S.G. ~2.7–2.8) to tourmalinite (S.G. ~2.8–2.9), a small volume loss must have accompanied tourmalinization in the study area, which also contributed to residual enrichment of immobile elements in the tourmalinites (e.g., O'HARA and BLACKBURN, 1989).

Discussion

Textural and geochemical data clearly document formation of the Orobic tourmalinites by the metasomatism of conglomerates and/or sandstones along and near basement-cover décollements. Geologic constraints outlined by ZHANG et al. (1994) show that the tourmalinites are unrelated to submarine-hydrothermal processes (e.g., SLACK et al., 1984; SLACK, 1993, SLACK, 1996), including syngenetic exhalation and subseafloor replacement. Formation of the Orobic tourmalinites involved the development of cryptocrystalline schorl-dravite (ZHANG et al., 1994) by boron metasomatism of aluminous clays, feldspars, and/or micas, in precursor sediments (see SLACK, 1993; SLACK et al., 1993). Based on the preservation of extremely fine-grained tourmaline in the tourmalinites, and on the observation of tourmaline breakdown in major shear zones elsewhere (SLACK and ROBINSON, 1990), we suggest that the Orobic tourmalinites formed from previously cataclasized conglomerates and/or sandstones. This model is similar to that proposed by BERG (1977) for tourmaline-rich protomylonites in the Bitterroot Range of southwestern Montana, in which preexisting mylonitic rocks were tourmalinized during the emplacement of nearby tourmaline pegmatite. It differs, however, from the model of LABERNARDIÈRE (1967), who proposed formation of a tourmaline-rich mylonite in the Massif Central by deformation of tourmaline-quartz veins related to a local leucogranite. The origin of cryptocrystalline blue tourmaline in a fault zone near Barstow, California (KRAMER and ALLEN, 1954) is unknown.

Mass change data suggest high fluid fluxes during tourmalinite formation. In geochemical studies of stratabound tourmalinites in the Broken Hill (Australia) district, SLACK et al. (1993) showed their formation to have involved, on average, major gain of B, minor gain of Mg and Na, major loss of Mn, Ca, and K, and minor loss of Si. In contrast are data for discordant tourmalinites in the large feeder zone of the Sullivan Pb–Zn–Ag deposit (British Columbia) that show major gain in B, Mg, and Mn and major loss of Ca, Na, and K (SLACK et al., 1996). Compositional differences between these two groups of tourmalinites are believed to reflect time-integrated water/rock ratios (i.e., fluid fluxes), in which the Broken Hill tourmalinites formed under relatively low water/rock conditions whereas the Sullivan tourmalinites formed under relatively high water/rock conditions (see also SLACK, 1996). Average mass changes calculated for the common (Group A) Orobic tourmalinites suggest that they formed under high water/rock conditions accompanied by moderate to significant loss of elements such as Ti, Cr, and the light REE. These same elements were mainly conserved during tourmalinite formation at Broken Hill (SLACK et al., 1993), but locally were lost at Sullivan, except for Ti that remained largely immobile (SLACK et al., 1996). Both the Broken Hill and Sullivan tourmalinites display general loss of Rb and Ba as in the Orobic tourmalinites (Fig. 6), but the major gain in Sr

shown by the Orobic tourmalinites is not characteristic of tourmalinites of submarine-hydrothermal origin (see BANDYOPADHYAY et al., 1993; SLACK et al., 1993, 1996).

The minor silica loss documented during formation of the Orobic tourmalinites is similar to that found by SLACK et al. (1993) at Broken Hill. This loss of SiO_2 reflects metasomatic changes during the replacement of clays, feldspars, and/or micas by tourmaline, in which quartz is generated as a product of various tourmaline-forming reactions. At Broken Hill, evidence of silica loss is shown by the local occurrence of siliceous haloes along tourmalinite-wall rock contacts (SLACK et al., 1993). Although such haloes have not been found surrounding the Orobic tourmalinites, geochemical data suggest introduction of silica into the underlying cover cataclasites, as these lithologic components contain high SiO_2 values (75.8 and 85.3 wt%) and high Si/Al ratios (5.64 and 10.8) that are much greater than those of their inferred conglomerate and/or sandstone protoliths (59.4–69.4 wt% and 2.38–4.57, respectively). The very high SiO_2 contents and Si/Al ratios of the basement gneisses in contact with tourmalinites (80.4–86.6 wt% and 6.12–10.8, respectively) clearly are not primary (e.g., granite) compositions, and probably reflect silicification during tourmalinite (or earlier cataclasite) formation. Related to this proposed silicification is an apparent net mass gain in the gneisses that produced low overall REE abundances (Fig. 4D). The source of the light REE concentrated in the tourmaline-poor cataclasites of the study area (Fig. 4B) may be locally derived from the conglomerate and/or sandstone precursors to the tourmalinites that show systematically larger Al-normalized ratios of light REE than the tourmalinites (Tab. 3).

The source of boron and other elements introduced into the tourmalinites is uncertain. ZHANG et al. (1994) suggested that these components were related to widespread development of tourmaline alteration at and near the Novazza and Val Vedello uranium mines, the latter containing abundant uraninite and minor sphalerite and molybdenite in fault zones along basement-cover contacts (see CADEL et al., 1987; FUCHS, 1989). A genetic link between the tourmalinites discussed here and the tourmaline-rich rocks at Novazza and near Val Vedello is further supported by the involvement of Mg and Na addition during their formation (Fig. 5; CADEL, 1986; CADEL et al., 1987), and by the presence of 22.8 ppm U in one of the Orobic tourmalinites (Tab. 2) and 226 ppm U in a cover cataclasite in direct contact with tourmalinite (C.W. Passchier and J.S. Zhang, unpub. data). According to FUCHS (1989), tourmaline alteration at the Novazza deposit formed during resurgent doming of the ash-flow caldera responsible for erupting ignimbrites of the Permian Collio Formation. This model is consistent with the timing of brittle normal faulting developed along the basement-cover contact, and with U–Pb and Pb–Pb ages of 249 and 240 Ma, respectively, obtained for the Val Vedello mineralization (SIMPSON et al., 1981 in CADEL, 1986). Enrichment of the tourmalinites in Be (Fig. 6), which is unknown in tourmaline-rich rocks of submarine-hydrothermal origin (SLACK et al., 1993, 1996), strongly suggests that the tourmalinizing fluids had a magmatic component. The Tertiary Adamello granites ~35 km to the east are unlikely candidates for having provided this component because they contain only rare accessory tourmaline and lack related tourmalinized country rocks (BIANCHI et al., 1970; CALLEGARI and DAL PIAZ, 1973); these granites also have K–Ar, Rb–Sr, and U–Pb ages of ~30–42 Ma (DEL MORO et al., 1985; HANSMANN and OBERLI, 1991) and postdate the Alpine structures that cut the tourmalinites (see ZHANG et al., 1994). More attractive is a connection to the late Hercynian Val Biandino plutonic complex ~25 km to the west, which contains tourmaline locally in granites and pegmatites, and pervasively in some contact metasomatic aureoles (DE SITTER and DE SITTER-KOOMANS, 1949; PASQUARÈ, 1967). However, this suite of plutons was emplaced at 286 ± 15 Ma based on K–Ar and Rb–Sr geochronology (DE CAPITANI et al., 1988; THÖNI et al., 1992), and would appear to be too old to have played a role in generating the Val Vedello mineralization and the tourmalinites described herein, assuming that the U–Pb and Pb–Pb ages cited above are correct and that the Val Vedello ores and our studied tourmalinites are contemporaneous. While evidence for an association with the Val Biandino plutons is thus problematic, geologic and geochemical data (especially Be) for the tourmalinites best support a link to late Hercynian felsic magmatism, or possibly to emplacement of Triassic (~238 Ma) alkaline intrusions and related hydrothermal activity like that recognized in the Southern Alps to the east (BORSI et al., 1968; BARTH et al., 1993). Future studies employing stable isotopes ($\delta^{18}O$, δD, $\delta^{11}B$) could test this magmatically-based hypothesis, and shed additional light on the source of the boron and other constituents in tourmalinites of the region.

Acknowledgements

We especially thank the USGS chemists who supplied most of the data for this study, including D.F. Siems, J.S. Mee, and B.W. King (XRF analyses), D.L. Fey (ICP-

AES analyses), M.J. Malcolm (ICP-MS analyses), and R.T. Hopkins (emission spectrographic analyses); T.G. Djie Kwee (Universiteit Utrecht) provided additional ICP-AES analyses, and T. Van Meerten (Interuniversitair Reactor Instituut, Delft) supplied INAA analyses. Slack also thanks R.B. Berg for discussions on tourmaline-rich mylonites in Montana, and Y. Fuchs for correspondence on tourmaline and boron alteration at the Novazza and Val Vedello mines. Zhang acknowledges A. Boriani for help during field work, and J.-K. Blom, J. Hegeman, and A. Simons for providing samples for study. The manuscript has been improved by the reviews of S. Barth, M.P. Foose, Y. Fuchs, and J.N. Grossman.

References

AGUE, J.J. (1994): Mass transfer during Barrovian metamorphism of pelites, south-central Connecticut. I: evidence for changes in composition and volume. Am. J. Sci. 294, 989–1057.

ARGAST, S. and DONNELLY, T.W. (1987): The chemical discrimination of clastic sedimentary components. J. Sed. Petrol. 57, 813–823.

BANDYOPADHYAY, B.K., SLACK, J.F., PALMER, M.R. and ROY, A. (1993): Tourmalinites associated with stratabound massive sulphide deposits in the Proterozoic Sakoli Group, Nagpur district, central India. In: MAURICE, Y.T. (ed.): Proceed. Eighth Quadr. IAGOD Symp., E. Schweizerbart'sche Verlagsbuchhandlung, Stuttgart, 867–885.

BARTH, S., OBERLI, F., MEIER, M., BLATTNER, P., BARGOSSI, G.M. and DI BATTISTINI, G. (1993): The evolution of a calc-alkaline basic to silicic magma system: geochemical and Rb–Sr, Sm–Nd, and $^{18}O/^{16}O$ isotopic evidence from the late Hercynian Atesina-Cima d'Asta volcano-plutonic complex, northern Italy. Geochim. Cosmochim. Acta 57, 4285–4300.

BAUMGARTNER, L.P. and OLSEN, S.N. (1995): A least-squares approach to mass transport calculations using the isocon method. Econ. Geol. 90, 1261–1270.

BERG, R.B. (1977): Reconnaissance geology of southernmost Ravalli County, Montana. Montana Bur. Mines Geol. Mem. 44, 39 pp.

BIANCHI, A., CALLEGARI, E. and JOBSTRAIBIZER, P.G. (1970): I tipi petrografici fondamentali del plutone dell'Adamello. Mem. Inst. Geol. Mineral. Univer. Padova 27, 148 pp.

BORSI, S., FERRARA, G., PAGANELLI, L. and SIMBOLI, G. (1968): Isotopic age measurements of the M. Monzoni intrusive complex. Miner. Petrogr. Acta 14, 171–183.

CADEL, G. (1986): Geology and uranium mineralization of the Collio basin (central Southern Alps, Italy). Uranium 2, 215–240.

CADEL, G., FUCHS, Y. and MENEGHEL, L. (1987): Uranium mineralization associated with the evolution of a Permo-Carboniferous volcanic field – examples from Novazza and Val Vedello (northern Italy). Uranium 3, 407–421.

CALLEGARI, E. and DAL PIAZ, G. (1973): Field relationships between the main igneous masses of the Adamello intrusive massif (northern Italy). Mem. Inst. Geol. Mineral. Univ. Padova 29, 38 pp.

CASSINIS, G. and PEROTTI, C.R. (1993): Interazione strutturale Permiana tra la linea delle Giudicarie ed i bacini di Collio, Tione e Tregiovo (Sudalpino centrale, N Italia). Boll. Soc. Geol. Ital. 112, 1021–1036.

CASSINIS, G., DAL PIAZ, G.V., EUSEBIO, A., GOSSO, G., MARTINOTTI, G., MASSARI, F., MILANO, P.F., PENNACCHIONI, G., PERELLO, M., PESSINA, C.M., ROMAN, E., SPALLA, M.I., TOSETTO, S. and ZERBATO, M. (1986): Report on a structural and sedimentological analysis in the uranium province of the Orobic Alps, Italy. Uranium 2, 241–260.

CONDIE, K.C. and SINHA, A.K. (1996): Rare earth and other trace element mobility during mylonitization: a comparison of the Brevard and Hope Valley shear zones in the Appalachian Mountains, USA. J. Metam. Geol. 14, 213–226.

DE CAPITANI, L., DELITALA, M.C., LIBORIO, G., MOTTANA, A., NICOLETTI, M. and PETRUCCIANI, C. (1988): K–Ar dating of the Val Biandino plutonic complex (Orobic Alps, Italy). Mem. Sci. Geol. Univ. Padova 40, 285–294.

DEL MORO, A., PARDINI, G., QUERCIOLI, C., VILLA, I.M. and CALLEGARI, E. (1985): Rb/Sr and K/Ar chronology of Adamello granitoids, Southern Alps. Mem. Soc. Geol. Italiana 26, 285–299.

DE SITTER, L.U. and DE SITTER-KOOMANS, C.M. (1949): The geology of the Bergamasc Alps, Lombardia, Italy. Leidse Geologische Mededelingen 14B, 1–257.

DIELLA, V., SPALLA, M.I. and TUNESI, A. (1992): Contrasting thermomechanical evolutions in the Southalpine metamorphic basement of the Orobic Alps (Central Alps, Italy). J. Metam. Geol. 10, 203–219.

FERRY, J.M. (1979): Reaction mechanisms, physical conditions, and mass transfer during hydrothermal alteration of mica and feldspar in granitic rocks from south central Maine, USA. Contrib. Mineral. Petrol. 68, 125–139.

FUCHS, Y. (1987): Zonalité des différents types de tourmaline dans le système hydrothermal de Novazza (Alpes Bergamasques, Italie du Nord). C.R. Acad. Sci. Paris 305(II), 1507–1510.

FUCHS, Y.A. (1989): Hydrothermal alteration at the Novazza volcanic field and its relation to the U–Mo–Zn Novazza deposit, northern Italy. In: Panel Proceed. Series, Metallogenesis of Uranium Deposits. Vienna, Inter. Atomic Energy Agency, 137–151.

FUCHS, Y. and MAURY, R. (1995): Borosilicate alteration associated with U–Mo–Zn and Ag–Au–Zn deposits in volcanic rocks. Min. Deposita 30, 449–459.

GIOBBI, E.O., BERNASCONI, A. and RAVAGNANI, D. (1981): Petrologic and metallogenic investigations on the Collio Formation of the Novazza uranium mine, Bergamasc Alps (Italy). Soc. Italiana Mineral. Petrol. 38, 293–305.

GUNDERSEN, L.C.S. and GATES, A.E. (1995): Mechanical response, chemical variation, and volume change in the Brookneal and Hylas shear zones, Virginia. J. Geodynamics 19, 231–252.

HANSMANN, W. and OBERLI, F. (1991): Zircon inheritance in an igneous rock suite from the southern Adamello batholith (Italian Alps). Contrib. Mineral. Petrol. 107, 501–518.

KERRICH, R., FYFE, W.S., GROMANN, B.E. and ALLISON, L. (1977): Local modification of rock chemistry by deformation. Contrib. Mineral. Petrol. 65, 183–190.

KRAMER, H. and ALLEN, R.D. (1954): Analyses and indices of refraction of tourmaline from fault gouge near Barstow, San Bernadino County, California. Am. Mineral. 39, 1020–1023.

LABERNARDIÈRE, H. (1967): Gisement, caractères et nature de quelques ultramylonites de la zone broyée d'Argentat (Corrèze). C.R. Acad. Sci. Paris 264(D), 1829–1832.

LAUBSCHER, H.P. (1985): Large-scale, thin-skinned

thrusting in the Southern Alps: kinematic models. Geol. Soc. Am. Bull. 96, 710–718.

MacLean, W.H. and Barrett, T.J. (1993): Lithogeochemical techniques using immobile elements. J. Geochem. Expl. 48, 109–133.

Marquer, D., Gapais, D. and Capdevila, R. (1985): Comportement chimique et orthogneissification d'une granodiorite en faciès schistes verts (Massif de l'Aar, Alpes centrales suisses). Bull. Minéral. 108, 209–221.

Milano, P.F., Pennacchioni, G. and Spalla, M.I. (1988): Alpine and pre-Alpine tectonics in the central Orobic Alps (Southern Alps). Eclogae geol. Helv. 81, 273–293.

Nakamura, N. (1974): Determination of REE, Ba, Fe, Mg, Na and K in carbonaceous and ordinary chondrites. Geochim. Cosmochim. Acta 38, 757–775.

O'Hara, K. and Blackburn, W.H. (1989): Volume-loss model for trace-element enrichments in mylonites. Geology 17, 524–527.

Pasquarè, G. (1967): Analisi geologico-strutturale del complesso intrusivo di Val Biandino (Alpi Orobie Occidentali). Mem. Soc. Geol. Italiana 6, 343–357.

Sawyer, E.W. (1986): The influence of source rock type, chemical weathering and sorting on the geochemistry of clastic sediments from the Quetico Metasedimentary Belt, Superior Province, Canada. Chem. Geol. 55, 77–95.

Schönborn, G. and Schumacher, M.E. (1994): Controls on thrust tectonics along basement-cover detachment. Schweiz. Mineral. Petrogr. Mitt. 74, 421–436.

Sibson, R.H. (1977): Fault rocks and fault mechanisms. Geol. Soc. London J. 133, 191–213.

Sinha, A.K., Hewitt, D.A. and Rimstidt, J.D. (1986): Fluid interaction and element mobility in the development of ultramylonites. Geology 14, 883–886.

Slack, J.F. (1993): Models for tourmalinite formation in the Middle Proterozoic Belt and Purcell supergroups (Rocky Mountains) and their exploration significance. Geol. Survey Canada, Current Res. Paper 93-1E, 33–40.

Slack, J.F. (1996): Tourmaline associations with hydrothermal ore deposits. In: Grew, E.S. and Anovitz, A.M. (eds): Boron: mineralogy, petrology, and geochemistry. Rev. Mineral. 33 (in press).

Slack, J.F. and Robinson, G.R., Jr. (1990): Retrograde metamorphic breakdown of tourmaline at Broken Hill, Australia. Geol. Soc. America Abs. Pgms. 22, 126.

Slack, J.F., Herriman, N., Barnes, R.G. and Plimer, I.R. (1984): Stratiform tourmalinites in metamorphic terranes and their geologic significance. Geology 12, 713–716.

Slack, J.F., Palmer, M.R., Stevens, B.P.J. and Barnes, R.G. (1993): Origin and significance of tourmaline-rich rocks in the Broken Hill district, Australia. Econ. Geol. 88, 505–541.

Slack, J.F., Shaw, D.R., Leitch, C.H.B. and Turner, R.J.W. (1996): Tourmalinites and coticules at the Sullivan Pb–Zn–Ag deposit and vicinity: geology, geochemistry, and genesis. In: Lydon, J.W., Höy, T., Slack, J.F. and Knapp, M.E. (eds): The Sullivan lead-zinc-silver deposit, Kimberley, British Columbia, and its geological environment. Geol. Survey Canada Bull. (submitted).

Thöni, M., Mottana, A., Delitala, M.C., De Capitani, L. and Liborio, G. (1992): The Val Biandino composite pluton: a late Hercynian intrusion into the south-Alpine metamorphic basement of the Alps (Italy). Neues Jahrb. Mineral. Monat. 12, 545–554.

Tobisch, O.T., Barton, M.D. and Vernon, R.H. (1991): Fluid-enhanced deformation: transformation of granitoids to banded mylonites, western Sierra Nevada, California, and southeastern Australia. J. Struct. Geol. 13, 1137–1156.

Zhang, J.S., Passchier, C.W., Slack, J.F., Fliervoet, T.F. and De Boorder, H. (1994): Cryptocrystalline Permian tourmalinites of possible metasomatic origin in the Orobic Alps, northern Italy. Econ. Geol. 89, 391–396.

Manuscript received March 25, 1996; minor revision accepted May 13, 1996.